RAA 2019 Vol. **19** No. **5**, 65(4pp) doi: 10.1088/1674–4527/19/5/65

http://www.raa-journal.org *http://iopscience.iop.org/raa*

***R**esearch in*
***A**stronomy and*
***A**strophysics*

C/2015 O1: A long-period comet with photometric observations ⋆

Xuan Zhang[1], Jin-Zhong Liu[1], Ya-Hui Wang[1,2] and Li-Na Lu[1,3]

[1] Xinjiang Astronomical Observatory, Chinese Academy of Sciences, Urumqi 830011, China; *liujinzh@xao.ac.cn*
[2] School of Physical Science and Technology, Xinjiang University, Urumqi 830046, China
[3] University of Chinese Academy of Sciences, Beijing 100049, China

Received 2018 October 24; accepted 2018 December 31

Abstract In this work, we report the observations of the long-period comet C/2015 O1 performed on 2018 January 29–30 and April 13 with the Nanshan 1-meter wide-field telescope operated by Xinjiang Astronomical Observatory. We obtain the morphological features of C/2015 O1 using an image enhancement method, and calculate the dust-activity parameter $Af\rho$ and the coma color based on photometric analysis. An obvious fan-shaped structure was observed at different observation times. We find that the activity of C/2015 O1 gradually decreases as the comet advances toward perihelion and the observed $B-V$ and $V-R$ colors are consistent with those of other comets.

Key words: comets: general — comets: individual (C/2015 O1)

1 INTRODUCTION

Comets are known to be very abundant in volatile ices and refractory dust grains. Long-period comets (LPCs) might form from the Oort Cloud (Meech & Svoren 2004). It was proposed that some other comets in the Oort Cloud may have an extrasolar origin (i.e., protoplanetary discs of other stars) (Levison et al. 2010). In addition, Meech et al. (2009) demonstrated that the models above exhibit a relationship between cometary activity and abundance and composition of trapped gas. Old LPCs are very scarce in the near-Earth region with $q < 2$ astronomical units (AU) as derived from observational features, which contradicts a uniform distribution of orbital energies on dynamical grounds (Oort & Schmidt 1951; Neslušan 2007). Levison et al. (2002) found that a comet would lose material via complicated processes (e.g., sublimation, outbursts, fragmentation and their ultimate disruption) during evolution from a new LPC to an old one. Due to solar radiation, the surface temperature of a comet increases when its distance is close to 3 – 4 AU from the Sun, which leads to ice sublimation in the coma (Lin et al. 2016). Therefore, when the comet approaches perihelion (closest to the Sun), its outgassing activity will increase (Wang et al. 2012).

Comet C/2015 O1 with a magnitude of 19.6 mag in the R band, following an orbit with an eccentricity of 0.999894 and an inclination to the ecliptic plane of 127.21°, was discovered by the Pan-STARRS 1 telescope (Haleakala) on 2015 July 19. This comet may have originated from the Oort Cloud, due to its long orbital period of 6 600 419.07 years. It reached perihelion on 2018 February 20 (MPC[1]) at a heliocentric distance of 3.517 AU. To date, apart from some normal imaging observations (see Seiichi Yoshida's home page[2]), few studies have focused on the morphology and multi-color observations of this comet.

In this work, we will present the imaging observations of comet C/2015 O1 in 2018 using Johnson-Cousins filters (e.g., Cousins 1976). The comet's orbital parameters are listed in Table 1 and its observation log is given in Table 2. The reminder of this paper is organized as follows. In Section 2 we describe the observations and data reduction for the comet C/2015 O1, and in Section 3 we give the results and discussion on the morphology, the $Af\rho$ parameter and the coma color for the comet.

2 OBSERVATIONS AND DATA REDUCTION

The observations were performed using the Nanshan 1-meter wide-field telescope (NOWT), operated by Xinjiang Astronomical Observatory. NOWT is equipped with an E2V 4k×4k CCD camera, a pixel scale of 1.125″ and a field of view (FOV) of 1.3° × 1.3° (Liu et al. 2014). The

⋆ A contributed paper of the International Symposium on Lunar and Planetary Science (ISLPS) on 2018 June 12–15 at Macau University of Science and Technology.

[1] Minor Planet Center: *https://www.minorplanetcenter.net*

[2] *http://www.aerith.net/index.html*

Table 1 Orbital Parameters of the Target Comet

Comet	a^a[AU]	e^b	q^c[AU]	i^d[°]	Peri^e[°]	Node^f[°]
C/2015 O1	35186.90	0.999894	3.73	127.21	89.61	299.86

Notes: ^{a} semimajor axis, ^{b} orbital eccentricity, ^{c} perihelion distance, ^{d} J2000 inclination, ^{e} J2000 argument of perihelion and ^{f} J2000 longitude of ascending node.

data were obtained from the B, V and R bands with a sequence of BVR,...,BVR. The effective wavelengthes are $\lambda_{\rm e} = 435.3$ nm, 547.7 nm and 435.3 nm for the B band, V band and R band, respectively, and the full-width at half-maximum (FWHM) values are $\Delta\lambda = 78.1$ nm, 99.1 nm and 106.56 nm for the B band, V band and R band, respectively. During the observations, the telescope was pointed toward the comet with non-sidereal motion.

By applying standard data reduction procedures (Song et al. 2016), we processed the data, beginning with bias subtraction and flat-field correction for all image frames. We obtained the bias value from an average of several zero-exposure frames. Flat-fields were chosen from the dithered images of twilight sky. To enhance the photometric precision of C/2015 O1, we selected a region far from the nucleus for background sky statistics using the PHOT package of IRAF, and did aperture photometry for all the CCD images. The following formulas were used to calibrate the magnitude of C/2015 O1

$$\begin{aligned} b - B = &-0.150(\pm0.006)(B-V) \\ &+0.278(\pm0.008)X_b + 2.137\,(\pm0.011)\,, \end{aligned} \tag{1}$$

$$\begin{aligned} v - V = &0.070(\pm0.013)(B-V) \\ &+0.210(\pm0.008)X_v + 2.415\,(\pm0.010)\,, \end{aligned} \tag{2}$$

$$\begin{aligned} r - R = &0.163(\pm0.013)(V-R) \\ &+0.158(\pm0.008)X_r + 2.238(\pm0.011)\,, \end{aligned} \tag{3}$$

where b, v and r are the instrumental magnitudes, B, V and R are the standard magnitudes, and X denotes airmass. Table 3 shows the photometric results for C/2015 O1. To provide absolute photometric calibration, we observed Landolt photometric standard stars (Landolt 1992) throughout the night. These observations give the zero-point, extinction coefficient and color term for each filter. The values are then used to calculate the magnitudes of the comet images. Each measurement uncertainty in Table 3 is derived from the transformation from instrumental to standard magnitude.

3 RESULTS AND DISCUSSION

Some different kinds of methods have been used to study the physical properties of comets (e.g., Lin et al. 2013). In the present work, what we are concerned with is investigating the activity of C/2015 O1 basd on three types of methods, including coma morphology, $Af\rho$ parameter and coma color.

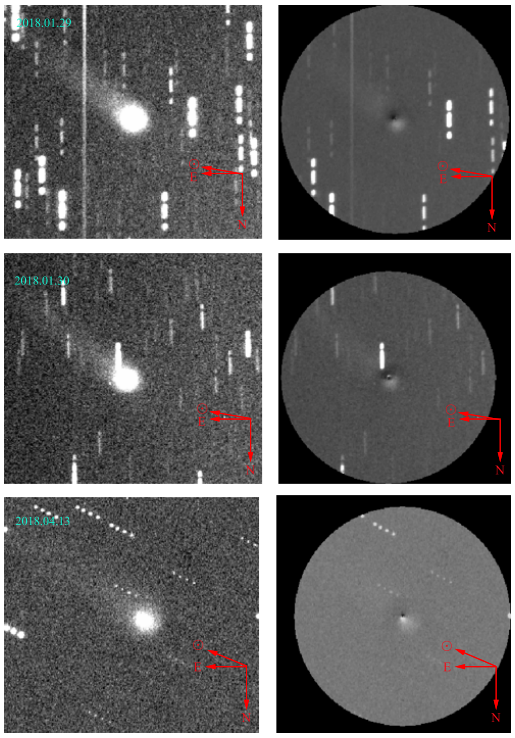

Fig. 1 Morphological analysis of R band images of comet C/2015 O1. The first column shows the original images and the second column displays the azimuthal median profile division of the final images. The first row, the second row and the third row feature the images of the R band taken on 2018 January 29, January 30 and April 13, respectively.

3.1 Coma Morphology

All morphological frames are obtained from the R band, which could be the most suitable for analyzing the dust coma morphology, compared with the gas emission bands (e.g., Birkle & Boehnhardt 1992; Fulle et al. 1993; Lara et al. 2009). Due to sufficient signal-to-noise ratio in our images, we use an image without stacking to analyze the coma morphology. In order to search for distinct characteristics associated with extended dust, we have explored the coma images using the method of azimuthal median profile division, which reduced the general coma background and enhanced faint coma structures.

Figure 1 exhibits a $300'' \times 300''$ region of the full frame that can be examined for investigating the inner coma of comet C/2015 O1. At first, we determine the azimuthal median profile division with the median brightness at radial distance from the nucleus of the cometary coma, then divide the comet image by the median brightness profile to enhance the structures of the coma. This method has been applied to all images taken in the R band. From Figure 1,

Table 2 Log of the Photometric Observations for C/2015 O1

UT date	$R_{\rm h}$[AU]	Δ (AU)	α (°)	Filter×Number	$T_{\rm exp}$ (s)	Pixel size (km)
2018–01–29	3.734	3.838	14.9	B×11,V×11,R×11	40	3133.2121
2018–01–30	3.734	3.833	14.9	B×17,V×17,R×16	40	3127.5005
2018–04–13	3.759	3.244	14.8	B×8,V×5,R×5,I×5	50	2646.9115

Notes: $R_{\rm h}$ is the heliocentric distance in AU, Δ is the geocentric distance in AU, α is the solar phase angle in degrees and $T_{\rm exp}$ is the total exposure time in seconds.

Table 3 Observational Results for C/2015 O1

UT date	ρ (arcsec)	B band (mag)	V band (mag)	R band (mag)	$B-V$	$V-R$	$Af\rho$ (cm)
2018–01–29	23.60	14.605±0.047	13.926±0.023	13.426±0.024	0.679 ±0.052	0.500±0.033	2580±56
2018–01–30	16.88	15.328±0.073	14.406±0.033	13.932±0.035	0.922±0.080	0.474±0.049	2189±71
2018–04–13	15.75	15.554±0.067	14.719±0.036	14.159±0.036	0.835±0.073	0.560±0.051	1686±54

Notes: B, V and R are the calibrated magnitudes of C/2015 O1, $B-V$ and $V-R$ are coma colors, ρ is the radius of photometric aperture, $Af\rho$ is obtained from the different aperture of ρ in the R band and the errors are derived from the photometric calibration.

we can see that there is a dust tail with a diffuse structure extending in the southeast quadrant. Moreover, an obvious sign in the anti-tail direction of the comet is the fan-shaped structure in the enhanced images. There is a relatively slight variation seen in the fan-shaped structure between 2018 January 29 and 30. The structure also appears in the image obtained on 2018 April 13. Note that more details of the dim part of the comet are not seen in the series of images because of the influence of moonlight.

The dust coma structure implies that there may be an active area on the comet's nucleus in the anti-tail direction. The region associated with the fan-shaped structure area still outflowing at pre-/post-perihelion. As can be seen from Figure 1, when the comet's heliocentric and geocentric distances decrease, the dust outflow becomes fainter. The dust tail is found in the approximate point of the solar direction. Based on our analysis, it is suggested that the slight variation of the coma may be caused by the rotation of C/2015 O1 (e.g., Bair et al. 2018), but there is no clear evidence to support this.

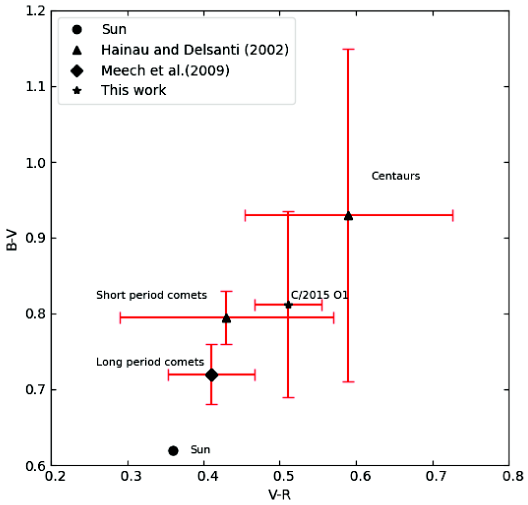

Fig. 2 $B-V$ color plotted against $V-R$ color for this work (*five-pointed star*) and other works (*triangles* or *diamond*). The color of the Sun is marked (*dot*).

3.2 $Af\rho$ Parameter

The $Af\rho$ value is usually used to describe the dust activity of a comet (Ahearn et al. 1984), where A is the average grain albedo, f is the filling factor of the aperture FOV and ρ is the linear aperture radius of the comet. The parameter $Af\rho$ is determined by

$$Af\rho = \frac{4R_h^2\Delta^2 10^{0.4(m_\odot - m_C)}}{\rho}, \qquad (4)$$

where r denotes the heliocentric distance, Δ denotes the geocentric distance, $m_\odot$ is the apparent magnitude of the Sun in the R band and m_c is the comet's integrated magnitude for the aperture radius m_c. The values of $Af\rho$ for comet C/2015 O1 were derived from data of the R band, as listed in Table 3. From this table, it can be seen that $Af\rho$ gradually decreased from 2580±56 cm to 1686±54 cm during 2018 January 29 to April 13.

The dust production rate among comets is usually signified by the parameter $Af\rho$, which represents some observational and physical parameters, such as the aperture size, geometric albedo of grains and so on (Mazzotta Epifani et al. 2011). The multi-aperture measurements reveal that $Af\rho$ is nearly constant (within error bars) outside $\phi = 15.75''$, which indicates a dust environment consistent with a situation of steady-state emission. The fluctuation of $Af\rho$ at different ρ implies that there may be non-steady-state dust emission from the coma (e.g., Shi et al. 2014).

3.3 Coma Color

The observational data obtained by NOWT allow us to perform an analysis of coma colors (at least partially) for C/2015 O1. The coma BVR magnitude and coma color at the selected aperture are displayed in Table 3. Based on this table, we can find that the color of C/2015 O1 in $V-R$ did not change by a statistically significant amount between January 29 and 30, but the color in $B-V$ did increase by a statistically significant amount, i.e., by $>3\sigma$. It might simply be that there were thin clouds on 2018 January 30 that absorbed more light in B band than in V and R bands. We make a plot of the corresponding broad-band colors $B-V$ versus $V-R$, as shown in Figure 2. The color index of the Sun is represented by a solid point, and its values are $B-V=0.62$ and $V-R=0.36$ (Drilling & Landolt 2000). The triangle stands for the color indices of the short-period comets (SPCs) and Centaurs (Hainaut & Delsanti 2002). In Figure 2, the values of the LPCs are obtained by averaging the observational results of Meech et al. (2009), in which an individual comet was observed using the same method of obtaining means and standard deviations so that the values are computed in the same way as those for the SPCs and Centaurs from Hainaut & Delsanti (2002).

Comparing the colors of C/2015 O1 with those of the Sun in Figure 2, it can be seen that the former is redder than the latter. Meanwhile, the colors of C/2015 O1 are closer to those of SPCs, since the values of the comet ($B-V=0.812$ and $B-V=0.795$) we obtained are closer to those ($B-V=0.795$ and $V-R=0.590$) of the SPCs. This phenomenon may originate from differences in dust properties or the activity level of C/2015 O1 (Storrs et al. 1992; Bonev et al. 2002; Jewitt 2009; Shi et al. 2014; Meech et al. 2016).

In this work, we present the observations of comet C/2015 O1 using NOWT and investigate its physical properties by the morphology method and photometric analysis. Our conclusions are summarized as follows:

(i) An elongated coma is displayed, and a scenario of dust outflow is depicted by an excess in the anti-tail direction.

(ii) The values of $Af\rho$ lie in the range of $1500\,\mathrm{cm} \leq Af\rho \leq 3000\,\mathrm{cm}$, which demonstrates that C/2015 O1 has dust activity to some extent.

(iii) An analysis of the diagram of $B-V$ versus $V-R$ shows that the colors of the LPCs and SPCs are not statistically different. Furthermore, the mean colors of C/2015 O1 are actually closer to those of the SPCs.

Acknowledgements This work was based on observations obtained at the Nanshan 1-meter wide-field telescope administered by Xinjiang Astronomical Observatory. We would like to thank Dr. Jianchun Shi for his help. The research was supported by the program of the light in China's Western Region (LCWR, Grant No. 2015-XBQN-A-02); the National Natural Science Foundation of China (Grant No. 11661161016); the 13th Five-year Informatization Plan of Chinese Academy of Sciences (Grant No. XXH13503–03–107); the Youth Innovation Promotion Association CAS (Grant No. 2018080); the Talent Importing Program offered by the government of Xinjiang Uygur Autonomous Region.

References

Ahearn, M. F., Schleicher, D. G., Millis, R. L., Feldman, P. D., & Thompson, D. T. 1984, AJ, 89, 579
Bair, A. N., Schleicher, D. G., & Knight, M. M. 2018, AJ, 156, 159
Birkle, K., & Boehnhardt, H. 1992, Earth Moon and Planets, 57, 191
Bonev, T., Jockers, K., Petrova, E., et al. 2002, Icarus, 160, 419
Cousins, A. W. J. 1976, MmRAS, 81, 25
Drilling, J. S., & Landolt, A. U. 2000, Normal Stars, ed. A. N. Cox, Allen's Astrophysical Quantities, ed. A. N. Cox (New York: AIP Press; Springer), 381
Fulle, M., Mennella, V., Rotundi, A., et al. 1993, A&A, 276, 582
Hainaut, O. R., & Delsanti, A. C. 2002, A&A, 389, 641
Jewitt, D. C. 2009, in European Planetary Science Congress 2009, 13
Landolt, A. U. 1992, AJ, 104, 340
Lara, L. M., Licandro, J., & Tozzi, G.-P. 2009, A&A, 497, 843
Levison, H. F., Duncan, M. J., Brasser, R., & Kaufmann, D. E. 2010, Science, 329, 187
Levison, H. F., Morbidelli, A., Dones, L., et al. 2002, Science, 296, 2212
Lin, Z.-Y., Lara, L. M., & Ip, W.-H. 2013, AJ, 146, 4
Lin, Z.-Y., Lai, I.-L., Su, C.-C., et al. 2016, A&A, 588, L3
Liu, J., Zhang, Y., Feng, G., & Bai, C. 2014, in IAU Symposium, 298, Setting the scene for Gaia and LAMOST, eds. S. Feltzing, G. Zhao, N. A. Walton, & P. Whitelock, 427
Mazzotta Epifani, E., Dall'Ora, M., Perna, D., Palumbo, P., & Colangeli, L. 2011, MNRAS, 415, 3097
Meech, K. J., & Svoren, J. 2004, Using Cometary Activity to Trace the Physical and Chemical Evolution of Cometary Nuclei, ed. G. W. Kronk, Comets II, ed. G. W. Kronk (Tucson: University of Arizona Press), 317
Meech, K. J., Pittichová, J., Bar-Nun, A., et al. 2009, Icarus, 201, 719
Meech, K. J., Sorli, K., Kleyna, J., et al. 2016, in AAS/Division for Planetary Sciences Meeting Abstracts, 48, 308.06
Neslušan, L. 2007, A&A, 461, 741
Oort, J. H., & Schmidt, M. 1951, Bull. Astron. Inst. Netherlands, 11, 259
Shi, J. C., Ma, Y. H., & Zheng, J. Q. 2014, MNRAS, 441, 739
Song, F.-F., Esamdin, A., Ma, L., et al. 2016, RAA (Research in Astronomy and Astrophysics), 16, 154
Storrs, A. D., Cochran, A. L., & Barker, E. S. 1992, Icarus, 98, 163
Wang, S., Zhao, H.-B., Ji, J.-H., et al. 2012, RAA (Research in Astronomy and Astrophysics), 12, 1576